Carbohydrate Polymers 336 (2024) 122120

Contents lists available at ScienceDirect

Carbohydrate Polymers

journal homepage: www.elsevier.com/locate/carbpol

Thermosensitive composite based on agarose and chitosan saturated with carbon dioxide. Preliminary study of requirements for production of new CSAG bioink

Adrianna Banach-Kopeć [a,1], Szymon Mania [a,*,1], Robert Tylingo [a], Agata Wawrzynowicz [a], Monika Pawłowska [b], Katarzyna Czerwiec [c], Milena Deptuła [d], Michał Pikuła [d]

[a] Department of Chemistry, Technology and Biotechnology of Food, Faculty of Chemistry, Advanced Materials Center, Gdańsk University of Technology, G. Narutowicza 11/12 Str., 80-233 Gdansk, Poland
[b] Department of Pharmaceutical Technology and Biochemistry, Faculty of Chemistry, Gdansk University of Technology, G. Narutowicza 11/12 Str., 80-233 Gdansk, Poland
[c] Division of Clinical Anatomy, Medical University of Gdańsk, M. Skłodowskiej-Curie 3a Str., 80-210 Gdańsk, Poland
[d] Laboratory of Tissue Engineering and Regenerative Medicine, Division of Embryology, Medical University of Gdansk, M. Skłodowskiej-Curie 3a Str., 80-210 Gdańsk, Poland

ARTICLE INFO

Keywords:
Agarose
Bioink
Biosafety, chitosan
3D printing, antimicrobial properties

ABSTRACT

This study introduces a method for producing printable, thermosensitive bioink formulated from agarose (AG) and carbon dioxide-saturated chitosan (CS) hydrogels. The research identified medium molecular weight chitosan as optimal for bioink production, with a preferred chitosan hydrogel content of 40–60 %. Rheological analysis reveals the bioink's pseudoplastic behavior and a sol-gel phase transition between 27.0 and 31.5 °C. The MMW chitosan-based bioink showed also the most stable extrusion characteristic. The choice of chitosan for the production of bioink was also based on the assessment of the antimicrobial activity of the polymer as a function of its molecular weight and the degree of deacetylation, noting significant cell reduction rates for *E. coli* and *S. aureus* of 1.72 and 0.54 for optimal bioink composition, respectively. Cytotoxicity assessments via MTT and LDH tests confirm the bioink's safety for L929, HaCaT, and 46BR.1 N cell lines. Additionally, XTT proliferation assay proved the stimulating effect of the bioink on the proliferation of 46BR.1 N fibroblasts, comparable to that observed with Fetal Bovine Serum (FBS). FTIR spectroscopy confirms the bioink as a physical polymer blend. In conclusion, the CS/AG bioink demonstrates the promising potential for advanced spatial cell cultures in tissue engineering applications including skin regeneration.

1. Introduction

Tissue engineering (TE) is a promising field that addresses the shortage of tissue donors and organs through the development of cellular scaffolds (Mandrycky, Phong, & Zheng, 2017). Several basic methods exist for producing materials for this industry, including solvent casting, particle leaching, freeze-drying, thermal-induced phase separation (TIPS), electrospinning, and gas foaming. However, significant potential lies in additive manufacturing techniques (Arifin, Sudin, Ngadiman, & Ishak, 2022). Among the available 3D printing techniques, such as fused deposition modeling (FDM), stereolithography (SLA), selective laser sintering (SLS), and bioprinting (BP), the latter appears most suitable in terms of the raw materials used and the microenvironment for living cells formed in a 3D functional object (Zaszczyńska, Moczulska-Heljak, Gradys, & Sajkiewicz, 2021). A key concept in tissue engineering is developing cell scaffolds that act as an artificial extracellular matrix (ECM) until new tissue forms, promoting cell survival, proliferation, and differentiation (Zhang et al., 2021). Recent scientific works demonstrate that the best ECM reproduction is achievable through the combination of BP technology and the use of natural

* Corresponding author.
E-mail addresses: adrianna.banach@pg.edu.pl (A. Banach-Kopeć), szymon.mania@pg.edu.pl (S. Mania), robertt@pg.edu.pl (R. Tylingo), s171385@student.pg.edu.pl (A. Wawrzynowicz), monika.pawlowska@pg.edu.pl (M. Pawłowska), katarzyna.czerwiec@gumed.edu.pl (K. Czerwiec), milena.deptula@gumed.edu.pl (M. Deptuła), michal.pikula@gumed.edu.pl (M. Pikuła).
[1] These authors contributed equally to this paper.

https://doi.org/10.1016/j.carbpol.2024.122120
Received 24 January 2024; Received in revised form 4 March 2024; Accepted 31 March 2024
Available online 2 April 2024
0144-8617/© 2024 The Authors. Published by Elsevier Ltd. This is an open access article under the CC BY-NC license (http://creativecommons.org/licenses/by-nc/4.0/).

polymer materials in hydrogel form (Chakraborty, Majumder, Sharma, Prasad, & Ghosh, 2022; Gao, Li, Liu, Huang, & Zhang, 2023; Himanshu, Sandeep, Avanish, & Shilpi, 2022; Wu et al., 2022). Bioprinting is the only method allowing for the distribution of living cells directly in the bioink and their precise embedding in the matrix, maintaining the cells' vital functions and high print resolution (Unagolla & Jayasuriya, 2020). Bioprinting live cell scaffolds requires meeting many criteria. Scaffolds must be biocompatible, biodegradable, non-cytotoxic, and mechanically stable. The size of the pores and the scaffold's porosity should facilitate gas exchange and the transport of nutrients and metabolites (Tan, Ngo, Sci, Leavesley, & Liang, 2022). The process also necessitates a rapid sol-gel phase transition (SGPT) that is non-invasive for cells, converting the bioink into a 3D bioprint during the creation of successive two-dimensional layers. This transformation's induction stems from the materials used for scaffold production and the phase transition effect may arise from physical factors like temperature or pH changes or chemical factors, such as using a coupling reagent (Innocenzi, 2020).

Marine organisms provide various polymers, including CS and AG, essential for tissue engineering. Compared to mammalian sources, they offer a lower risk of transmitting infectious diseases compared to mammalian sources. This is due to the lower biological relationship between humans and marine organisms, which reduces the possibility of cross-transmission of pathogens. The use of marine-derived materials avoids potential religious and cultural restrictions associated with the use of products derived from mammals such as pigs or cattle, which may be important in the context of the global use of biomaterials (Zhang et al., 2019). Chitosan is a cationic polymer constructed from β-1,4 glycosidic bonds of D-glucosamine and *N*-acetyl-d-glucosamine, derived from chitin through the deacetylation process. Chitin's primary sources are marine invertebrates' exoskeletons, insects, and fungi cell walls. Chitosan is bioactive, biocompatible, and biodegradable, possessing anticancer and antioxidant effects (Rinaudo, 2006). Due to amino groups in its structure, it also has antimicrobial properties (Cheung, Ng, Wong, & Chan, 2015). Consequently, chitosan is insoluble in water, solutions with a pH above 7, and most organic solvents. However, in acidic solutions, chitosan's amino groups become protonated, and the molecules dissolve. This fact significantly limits chitosan's use, especially in tissue engineering, due to the acid's toxic effect on living cells, reducing the material's biocompatibility. Another disadvantage of chitosan, despite its promising properties, is its poor printability and limited mechanical properties (Sadeghianmaryan et al., 2020). Thus, it's common to combine it with other polymers, like agarose, to enhance its properties. Agarose is a polysaccharide extracted from seaweed and algae, consisting of alternating D-galactose and 3,6-anhydro-L-galactopyranose linked by α-(1 → 3) and β-(1 → 4) glycosidic bonds (Salati et al., 2020). Unlike chitosan, agarose has a low capacity for promoting cell adhesion but can gel swiftly in a narrow temperature range, optimal for most living cells without requiring cross-linking agents (Zarrintaj et al., 2018). Additionally, the gel remains mechanically stable at physiological temperatures due to phase transition hysteresis, making agarose's primary bioprinting applications its use as a support material for other bioprinting components (Gu et al., 2020).

Only two solutions exist in the literature regarding bioink production using chitosan and agarose. Gu and co-authors presented a bioink based on carboxymethyl chitosan, agarose, and sodium alginate for the proliferation and differentiation of induced pluripotent stem cells from three germ layers—endoderm, ectoderm, and mesoderm (Gu et al., 2020). Bioprinting with these polymers relies on alginate cross-linking using calcium ions in the egg-box model. Butler and co-authors proposed a thermosensitive bioink based on *N*,*O*-carboxymethyl chitosan and agarose. Here, agarose stabilizes subsequent bioprint layers through sol-gel transformation resulting from bioink cooling (Butler, Naseri, MacDonald, Tasker, & Ahmadi, 2021). The *N*,*O*-carboxymethyl chitosan base's good water solubility eliminates the acid from the system, enhancing its biocompatibility. However, derivatization requires organic solvents and is time-intensive. Inadequate derivative purification might lead to cytotoxic effects. The presence of acid in the chitosan-agarose composite system is a significant limitation, as it hinders the composite's gelation, considerably prolongs its gelation time, or produces gels with weak mechanical properties. Due to these constraints, using the chitosan-agarose hydrogel composite in additive manufacturing is unfeasible, as it doesn't support the rapid formation of successive two-dimensional object layers (Graham, Marina, & Blencowe, 2019; Gu et al., 2020).

According to the research hypothesis, the use of chitosan hydrogel obtained as a result of CO_2 saturation and agarose hydrogel will enable the creation of a thermosensitive chitosan-agarose composite without the need for modification of either polymer, meeting the basic rheological and biological requirements to function as the main ingredient of bio-inks dedicated to bioprinting technology. In this approach, an unstable over time chitosan hydrogel formed by saturating carbon dioxide in an aqueous suspension containing microcrystalline sediment of this polymer, with a pH of ~6.5, is used. The concept of this idea is described in one of our previous works (Gorczyca et al., 2014). The higher pH value of materials based on chitosan devoid of acids significantly increases its application potential and removes many barriers related to the design of antimicrobial chitosan materials, which has been confirmed by our earlier works (Mania et al., 2018; Tylingo, Kempa, Banach-Kopeć, & Mania, 2022).

This publication, as the first in the scientific literature, presents a thermosensitive CSAG composite dedicated to bioprinting technology, which has antibacterial properties, does not cause a cytotoxic effect. Moreover, its production is based on the use of unmodified chitosan and agarose polymers, whose participation in the composite determines the sol-gel transition temperature. This material seems to be a universal medium for culturing many different cell lines.

2. Experimental

2.1. Materials

Chitosan (CS) with low (20–300 cps, DD ≥ 75 %, Cat. No.:102473649, LOT: BCCG5629), medium (200–800 cps, DD ≥ 75 %, Cat. No.:102466463, LOT: BCCG9377), high (800–2000 cps, DD ≥ 75 %, Cat. No.:102515456, LOT: BCCH4876) MW, chitosan isolated from crab (Cat. No.:101167160, LOT: BCBH3811V) and shrimp shells (DD ≥ 75 %, Cat. No.:1003507957, LOT: SLCP5257), and agarose (AG) with low EEO, 34.5–37.5 °C gel point, phosphate buffer saline (PBS) triptic soy agar (TSA), triptic soy broth (TSB), sodium chloride, peptone K, and glycolic acid were purchased from Merck (Germany). Sodium hydroxide was produced by Avantor Performance Materials Poland S.A (Gliwice, Poland). The carbon dioxide used to saturate the chitosan precipitate was derived from Linde Gaz Polska Sp. z o. o. (Gdańsk, Poland). For microbiological tests, the following bacterial strains were used: Gram (−) *Escherichia coli* (ATCC 25922) and Gram (+) *Staphylococcus aureus* (ATCC 29213) from the Polish Collection of Microorganisms, Ludwik Hirszfeld Institute of Immunology and Experimental Therapy of the Polish Academy of Sciences (Wrocław, Poland). Mouse fibroblast L929 cells were purchased from the American Type Culture Collection (ATCC, Manassas, VA, USA). Immortalized human keratinocyte HaCaT cells were purchased from the German Cancer Research Center (DKFZ, Heidelberg, Germany). Human skin fibroblast cell line 46BR.1 N obtained from the European Collection of Authenticated Cell Cultures (ECACC, Sigma Aldrich, St. Louis, MO, USA). The 3-(4,5-dimethylthiazol-2-yl)-2,5-diphenyltetrazolium bromide (MTT), Low-glucose Dulbecco's modified Eagle's medium (DMEM), antibiotics, and supplements necessary for cell culture were obtained from Sigma-Aldrich (St. Louis, MO, USA). Fetal bovine serum (FBS) was purchased from Biowest (Nuaille, France), MilliQ water was used for the preparation of all aqueous solutions. All other reagents were of analytical grade or higher.

The chitosans used in this work were thoroughly characterized in terms of molecular weight and degree of deacetylation in our previous

MOST WIEDZY Downloaded from mostwiedzy.pl

work. The table below summarizes these characteristics (Table 1).

2.2. CSAG composite bioink preparation

CS was dissolved in 0.1 M hydroxyacetic acid at a concentration of 1.5 % (*w*/w) with using mechanical stirrer at 200 RPM (RA 2020, Heidolph Instruments GmbH & Co. KG, Kelheim, Germany) until a homogeneous solution with no undissolved solids was obtained. To prepared CS solution, during mixing, 0.5 M solution of sodium hydroxide was added until the pH value in the range of 9–10 was reached. This was equivalent to complete precipitation of chitosan in the microcrystalline form. The precipitated chitosan was filtered with the use of vacuum filtration kit and washed several times with distilled water until the pH of the rinsing water reached a value equal 7.0. Finally, the precipitated chitosan was weighed and suspended in such an amount of distilled water to obtain a solution of 1 % (*w/v*) in relation to the dry matter of the polymer. The CS suspension was homogenized at 10000 RPM for 3 min (Silent Crusher M, Heidolph Instruments GmbH & Co. KG, Kelheim, Germany) and then saturated with CO_2 with simultaneously mechanical mixing using of with a hollow shaft stirrer for gas saturation (BIOMIX BMX-10, Gdańsk, Poland). Saturation and mixing were carried out until a homogeneous and transparent solution was obtained. This was a sign of complete dissolution of the CS.

A 1 % (m/m) AG solution was prepared as follows. AG was added in portions to water at 80 °C while maintaining stirring at 200 RPM (RA 2020, Heidolph Instruments GmbH & Co. KG, Kelheim, Germany) until the polymer was completely dissolved. Composites of CS and AG hydrogels were prepared by pre-cooling the hot AG solution to 45 °C and quickly combining it with the CS solution prepared according to the above description using a mechanical stirrer at 300 RPM for 2 min (BIOMIXBMX-10, Gdańsk, Poland), in this way so that the temperature of the polymer mixture does not drop below 40 °C until rheological and extrusion force measurements begin. To carry out FTIR tests and biological tests, CS, AG and their composites were frozen at −24 °C and then freeze-dried for 72 h ($p = 0.94$ mbar, sample temperature 20 °C, condenser temperature − 80 °C; Christ Alpha 12–4 LD Plus, Osterode am Harz, Germany).

2.3. Rheological properties

Rheological factors of the compositions affecting printability were investigated with the help of a Brookfield *V*iscometer (Brookfield DV-III Ultra AMETEK rheometer, Warsaw, Poland). Time and temperature of the SGPT, measurement of flow curves (FC) were investigated. SGPT was determined by measuring changes in the dynamic viscosity of the AG solution or CSAG bioinks during temperature changes in the range of 40–20 °C, at a cooling rate of 1 °C min^{-1} and at 5 rpm, on an SC4–25 spindle. The FC were determined by measuring the relationship between dynamic viscosity of AG solution or CSAG bioinks and shear rate at 37 °C. The shear rate was measured with SC4–25 spindle in the range of 0.1/s to 25.0 s^{-1}.

Table 1
Description of the tested chitosan samples, their DD and MW (n = 3, p < 0.05) (Mania et al., 2023). Values marked with different letters in each column differ significantly.

Seller chitosan name	DD [%]	MW [kDa]	Given symbol
Low molecular weight	75.7 ± 5.7a	89 ± 4a	LMW
Medium molecular weight	81.7 ± 4.8a	280 ± 10b	MMW
High molecular weight	78.8 ± 1.5a	591 ± 26c	HMW/H79
From shrimp shells*	66.2 ± 3.1c	545 ± 22c	HMW/H66
From crab shells*	83.2 ± 4.6b	4000 ± 142d	HMW/H83

* High molecular weight chitosan.

2.4. Extrusion force test

The extrusion force test (EFT) required to extrude the hydrogel composition were carried out on a universal testing machine (Instron model 5543 with "Merlin" V 4.42. software, Warsaw, Poland). First, extrusion tests were carried out for the 100 % AG system, in order to select from among three needles with 840, 580, 410 μm outlet diameters, the one with which further extrusion tests were carried out. For this purpose, a 60 mL syringe was filled with the appropriate ink and placed in a holder with a heating mat attached. The total volume of ink in the cartridges was 30 mL, and the incubation time at 37 °C to stabilize the temperature throughout the syringe volume was 10 min. The syringe plunger was then pushed down at a constant displacement speed of 0.25 mm/s, until all the ink was extruded from the syringe.

2.5. Antimicrobial activity

The evaluation of the antimicrobial properties of the materials was conducted according to the ASTM E2149 method with slight modifications using *E. coli* and *S. aureus* strains. Bacterial colonies were first subcultured in TSB and incubated for 24 h at 37 °C. Microbial suspensions were prepared in the test medium by adjusting the bacterial cell count to between 1.5×10^7 and 5×10^7 CFU/mL with a spectrophotometer (Merck Spectroquant Pharo 100, Germany) by measuring the absorbance at a wavelength of 600 nm (optical density between 0.08 and 0.1). To determine the antimicrobial activity of composites, 4 cm squares were cut from the test materials. The materials were sterilized under UV radiation for 30 min on each side. Subsequently, 0.4 mL of the inoculum was applied to each square. Immediately after inoculation, the materials labeled as '0 h exposure time' were transferred to 10 mL of PBS solution and shaken five times for 5 s using a vortex. Ten-fold serial dilutions and inoculations on TSA medium were performed. Plates were incubated for 24 h at 37 °C. The remaining materials labeled as '24-h exposure time' were incubated with the inoculum at 37 °C for 24 hs (Heidolph Incubator 1000, Merck Sp. z o.o., Warsaw, Poland), after which the same procedure was followed as for the '0 hs exposure time'. After incubation, bacterial colonies that grew on the Petri plates were counted. To calculate the number of cells per mL of the initial suspension, the results from the colony counts were used, with numbers ranging from 30 to 300 units, according to the equation:

$$Vc = N \times D,$$

where Vc is the bacteria concentration, in colony forming units per mL (CFU/mL), N is the average value, in colony forming units (CFU), from Petri dishes, D is the dilution factor from the plates counted. Antimicrobial activity was calculated according to the formula:

$$R = loglog\ \frac{B}{C},$$

where B is the average of the number of viable cells on the control sample after 24 h incubation at 37 °C (CFU/mL), C is the average of the number of viable cells on the tested sample after 24 h incubation at 37 °C (CFU/mL). A percentage reduction of bacteria/fungi on a logarithmic scale (R) equal to 1, 2, and 3 corresponds to a reduction of 90 %, 99 %, and 99.9 %, respectively.

2.6. Cytotoxicity against L929

2.6.1. Cell culture

Adult mouse fibroblast L929 cells were purchased from the American Type Culture Collection (ATCC, Manassas, VA, USA) and tested negative for mycoplasma using a Universal Mycoplasma Detection Kit (ATCC, Manassas, VA, USA). The L929 cell line was cultured in DMEM supplemented with 10 % heat-inactivated FBS, 100 μg/mL streptomycin, and 100 U/mL penicillin. Cells were incubated at 37 °C in a 5 % CO_2

MOST WIEDZY Downloaded from mostwiedzy.pl

atmosphere. All experiments were performed using cells in the exponential phase of growth.

2.6.2. Cell viability and morphology assessment

To estimate the in vitro cytotoxicity of the extracts, MTT assay was used, according to ISO 10993–5:2009(E). Briefly, L929 cells were seeded in 96-well plates at a density of 1×10^4 cells/well and 100 μL of culture medium (blank) was dispensed into the peripheral wells. After 24 h of incubation at 37 °C in a 5 % CO_2 atmosphere, the culture medium was removed and replaced with either fresh medium (positive control and blank) or fresh medium containing samples (1:1 *v*/v, 1:5 v/v, and 1:9 v/v of chitosan or agarose extract). Samples for cytotoxicity studies were prepared by suspending 0.1 g of the CS or AG xerogel in 10 mL of DMEM for 24 h at 37 °C. After this time, the liquid part of the sample (extract) was passed through a 0.22 μm filter. Following 24 h incubation, images of cells were taken using a 20× objective in an OLYMPUS I × 83 inverted microscope with an XC 50 camera and cellSens Dimension software. The culture medium was then removed, and 50 μL of the MTT solution (1 mg/mL in medium without supplements and phenol red) was added to each well and incubated for 2 h at 37 °C in a 5 % CO_2 atmosphere. Next, the MTT solution was removed, and the formazan crystals were dissolved in 100 μL isopropanol and shaken for 10 min. Absorbance was measured at 540 nm using a microplate reader (iMarkTM, Bio-Rad, Hercules, CA, USA). The results were obtained from four independent experiments ($n = 4$).

2.7. Biocompatibility analysis with XTT and LDH and live-dead assays

2.7.1. Cell culture

Analysis of biocompatibility was performed with the use of human cell lines: HaCaT keratinocytes (ATCC, Manassas, VA, USA) and 46BR.1 N fibroblast (ECACC, Sigma Aldrich Co.) Cells were routinely cultured in 25 cm^2 T-flask in standard conditions (5%CO_2, 37 °C) in DMEM HG medium (Sigma Aldrich) supplemented with 10 % FBS and antibiotics (100 U/mL of penicillin and 100 μg/mL streptomycin). Cells were passaged twice a week.

2.7.2. Extract preparation

The analysis was performed according to ISO 10993-5:2009 standard by the evaluation of extract activity. Extracts were prepared by incubation of xerogels (25 mg per 1 mL of culture medium) with DMEM HG culture medium for 24 h in 37 °C. After the time of incubation, the medium was collected, centrifuged (1500 rpm) and immediately used for cell stimulation. The following concentrations of extracts were used for cell stimulation: 100 % (undiluted) and 50, 25, 10 % (diluted with DMEM HG medium).

2.7.3. Cytotoxicity (LDH) and cell proliferation (XTT) assay

Lactate dehydrogenase (LDH, Roche) and XTT (Roche) tests were used to analyze cytotoxicity and the effect on cell viability respectively. Cells were seeded into 96-well plates (5000 cells per well) in DMEM HG medium with 10 % FBS and placed in standard condition for 24 h. Next, the medium was changed for extracts prepared by incubation of DMEM HG medium with xerogels. In both tests, cells cultured in DMEM HG medium constituted negative control. Cells cultured with DMEM HG supplemented with 10 % FBS and cells stimulated with 1 % TRITON X-100 (maximum cytotoxicity) were used as positive controls in XTT and LDH assay respectively. After 24 h hs of incubation, both tests were performed according to the manufacturer's instructions.

2.7.4. Live-dead assay

To investigate the efficacy of the newly developed bio-ink in maintaining cell viability, an experiment was conducted using a mixture of chitosan (1 % *w/v*) of medium molecular weight and agarose (1 % w/v) in a 1:1 ratio, and agarose (1 % w/v) alone as a control. These components were combined in equal proportions and incubated at 37 °C to prevent the composition from gelling. Cells, at a concentration of 1×10^6 cells/mL, were integrated with the prepared bio-ink and then applied to 24-well culture plates using a syringe, forming 3D structures. After the scaffolding gelled at temperatures below 37 °C, the wells were filled with the appropriate medium and placed in an incubator (37 °C, 5 % CO_2). To assess the cell viability in the produced structures after two days of incubation, selective staining was conducted to stain live cells green and dead cells red. After the removal of the medium, the scaffolds were cleansed with phosphate-buffered saline. Then, 3 mL of PBS solution with the addition of calcein and propidium iodide was added to each well. The incubation of scaffolds with the dyes was carried out in darkness at a constant temperature of 37 °C in a 5 % CO_2 environment for a period of 45 min. After incubation, the staining solution was removed, and observations were made using fluorescence microscopy (Nikon Eclipse TE300).

2.8. Chemical structure

FT-IR spectra of freeze-dried composite samples have been recorded using a spectrometer (Nicolet 8700; Thermo Electron Corp., Waltham, MA, USA) equipped with GoldenGate (Specac Corp., Oprington, UK) with a single-reflection diamond. The temperature of the crystal was maintained at 25.0 ± 0.1 °C during measurement. 64 scans were obtained with a resolution of 4 cm^{-1} within the wavelength range from 4000 to 550 cm^{-1}. The spectrum of each material was measured, averaged and corrected by background removal. Spectragryph *V* 1.2.10 software was used to process the obtained spectra (Oberstdorf, Germany).

2.9. 3D bioprinting

The printability of the thermosensitive CSAG bioink was verified empirically using the syringe heating system (37 °C) of the CSAG 3D bioprinter created as part of the DEC-10/2021/IDUB/I.3.3 project in Faculty of Chemistry, Gdańsk University of Technology. A detailed description can be found in supplementary materials. Subsequently, the samples were imaged using the TOP Show 3D automatic rotation system (Wroclaw, Poland).

2.10. Statistical analysis

The Prism 10 V10.0.3 (GraphPad software, Boston, MA, USA) was used for analyzing the results. The statistical significance was determined at $p < 0.05$. All data reported were based on the means of three replicates ($n = 3$) or four ($n = 4$) replicates in case of MTT tests. Experimental results were expressed as mean ± standard deviation (SD). The differences were considered to be statistically significant at $p < 0.05$. Statistical analysis of biocompatibility cell culture date was performer with one-way ANOVA ($p < 0.05$) and Mann-Whitney *U* test, ($p < 0.05$) in case of LDH and XTT tests.

3. Results and discussion

The results below present the only way to use chemically unmodified chitosan as a component of a universal cellular bioink, which can be successfully used in new research paths related to tissue regeneration (Ramiah, du Toit, Choonara, Kondiah, & Pillay, 2020).

3.1. Rheological evaluation

The main components of the developed composite as a potential bioink are CS and AG, where the second component is a factor ensuring its gelation. In order to determine the share of both polymers in the composite and the type of chitosan in terms of molecular weight, rheological tests were carried out SGPT (Fig. 1A), FC (Fig. 1B) and EFT (Fig. 2).

MOST WIEDZY Downloaded from mostwiedzy.pl

A

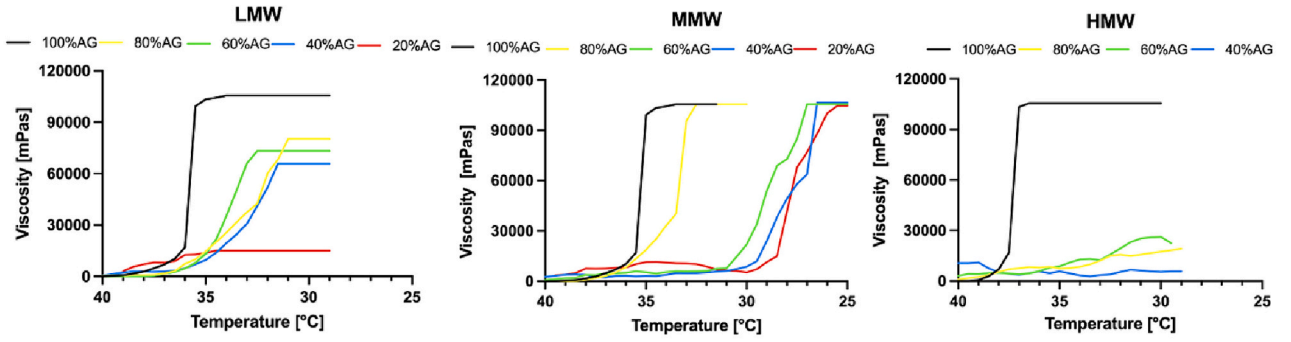

Sample	SGPT temperature range [°C]		Viscosity after SGPT [mPas]
100%AG	36.0	36.5	105557 ± 467
80%AG	31.5	36.5	80249 ± 76
60%AG	33.7	36.5	73136 ± 65
40%AG	32.6	36.7	65746 ± 72
20%AG	-	-	15068 ± 58

Sample	SGPT temperature range [°C]		Viscosity after SGPT [mPas]
100%AG	36.0	36.5	105557 ± 467
80%AG	33.1	36.5	105557 ± 289
60%AG	27.5	31.5	105602 ± 355
40%AG	27.0	30.5	105598 ± 402
20%AG	26.5	30.5	105623 ± 381

Sample	SGPT temperature range [°C]		Viscosity after SGPT [mPas]
100%AG	36.0	36.5	105557 ± 467
80%AG	-	-	19131 ± 87
60%AG	-	-	22459 ± 122
40%AG	-	-	5374 ± 140
20%AG	-	-	-

B

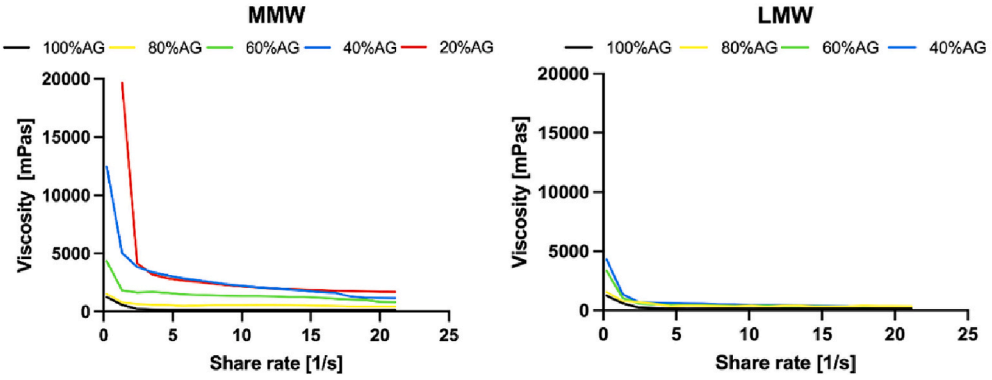

Fig. 1. Rheological properties of CSAG composition for chitosans of different molecular weights: low (LMW), medium (MMW), and high (HMW). (A) The rheological characteristic of the sol-gel phase transition and (B) flow curves of the CSAG composites ($n = 3$, $p < 0.05$).

Fig. 1 shows the results of the measurement of the sol-gel phase transition characteristics of hydrogels differing in the share of chitosan and agarose, which was performed for chitosan with low (LMW), medium (MMW), and high molecular weight (HMW). A clear influence of chitosan on the phase transition of the CSAG composite can be observed. SGPT for agarose begins at 36.5 °C and occurs the fastest - the lowest slope of the curve and the sharpest increase in viscosity caused by gelation of this polymer. Composites based on AG and LMW CS begin to gel at the same temperature as pure agarose, but the temperature range of their phase transition is much wider than for pure agarose (from 3 to 5 °C). The intrinsic viscosity of the sol measured before complete gelation decreased with the increase in the proportion of LMW CS in composite (Fig. 1A). For the HMW CSAG composite, no sharp phase transition was recorded, but only a slight increase in the viscosity during measurements for samples containing from 20 % to 60 % of CS hydrogel. It was impossible to perform measurements for the HMW CSAG composite marked as 20%AG. The most predictable SGPT characteristics were obtained from AG and CS of medium molecular weight. In this system, the increase in the share of chitosan in the composite did not affect the value of the intrinsic viscosity before gelation of the composite and caused a decrease in the temperature range in which it occurred.

Huang et al. (2018) in their studies of the phase transition temperature of two-component hydrogels prepared using CS and AG in the presence of 1 % citric acid demonstrated the same relationships. Compared to pure AG (0.5 °C), the gelation temperature of MMW CS based composites was in the range of 3.4–4 °C (Fig. 1A.). The gelation process during the cooling of pure agarose samples contains two major steps. The first is the formation of double helices upon cooling. So called "hardening step" at around 45 °C is assigned to the formation of "cross-links", i.e., the helices. Further hardening in the temperature range around 30 °C is likely to correspond to the aggregation of several helices (Nordqvist & Vilgis, 2011). The decrease in the viscosity of the sol before complete gelation with an increase in CS molecular weight suggests that LMW CS may interfere with the formation of agarose helices, leading to a more gradual and extended gelation process. In the case of HMW CS, the larger CS molecules interfere more significantly with the AG network formation, possibly by steric hindrance or by forming less efficient cross-links with AG. This effect disrupts the typical two-step gelation process of AG, leading to a less defined phase transition. In turn, MMW CS may facilitate more ordered or efficient packing of agarose molecules into helices and their subsequent aggregation and shift this process towards lower temperatures.

Due to the fact that HMW CSAG composites do not show a sharp SGPT, LMW and MMW CSs were used for further investigations (Figs. 1B, 2). Fig. 1B shows the viscosity of CSAG composites decreases exponentially with the increase in the shear rate, showing that in all

MOST WIEDZY Downloaded from mostwiedzy.pl

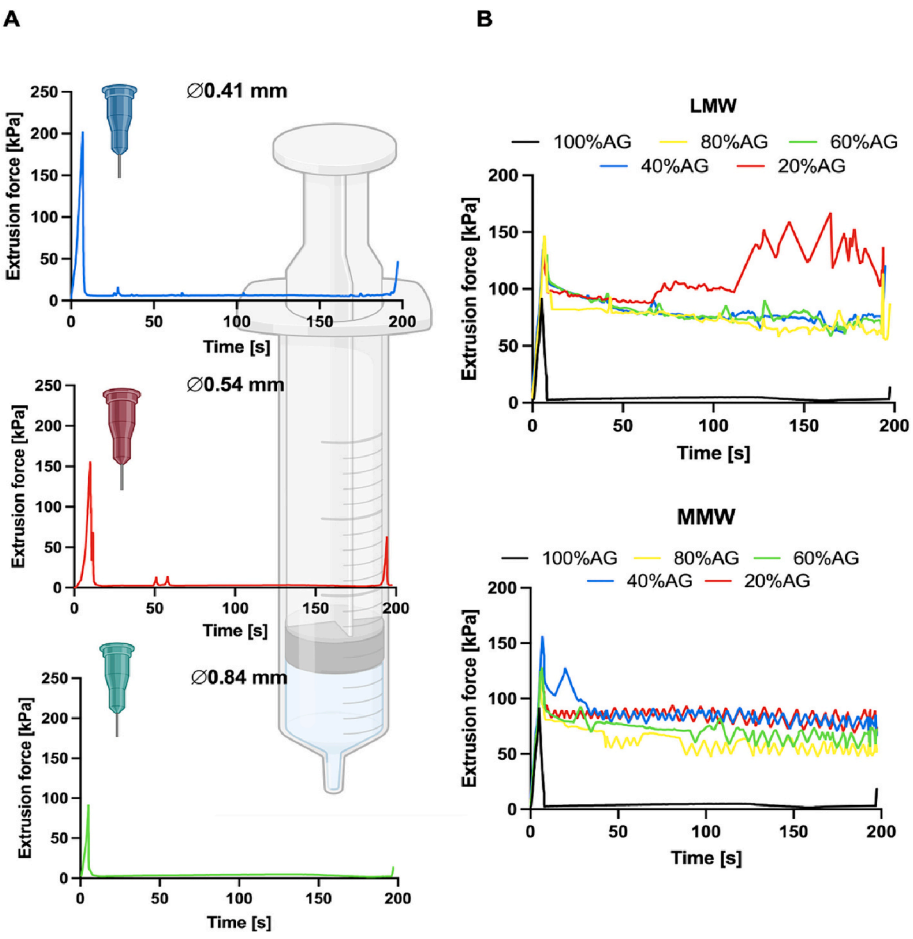

Fig. 2. The result of extrusion force test for (A) 1 % AG solution and (B) CSAG composites at 37 °C (n = 3, $p < 0.05$).

cases the fluids are pseudoplastic. The shear thinning effect of the CSAG composites is identical to that of CS hydrogels alone, i.e., both CSs (LMW and MMW) in the composites show shear thinning, but the degree of viscosity reduction under shear stress is less pronounced for low molecular weight chitosan than for the MMW variant. It also decreases with increasing agarose content in the CSAG composites. The explanation for this behavior is given in terms of the destruction of polymeric entanglement with consequent alignment of the chains in the direction of the shear flow (do Amaral Sobral et al., 2022). For all tested systems, it is possible to quickly achieve a steady flow of the potential bioink. A clear decrease in viscosity is observed after exceeding a shear rate of 3 1/s. The low shear rate will ensure easier flow control during printing and high cell viability, as the action of shear forces leads to cell disintegration (Smith & Doe, 2022).

The charts in Fig. 2 present the relationships of the extrusion force of polymeric hydrogels as a function of time. Section A pertains to the comparison of the extrusion curve for a 1 % AG solution at 37 °C, from a syringe ending in needles of 3 different diameters.

All charts are characterized by an initial rapid increase in the extrusion force necessary for thinning the system and initiating flow, which is typical for pseudoplastic fluids (Doe & Smith, 2021). After reaching the maximum value, the extrusion force drops sharply and stabilizes, suggesting that the material flows more easily through the nozzle after overcoming the initial resistance. The peak height decreases with the increase in needle diameter. The curves around 200 s of the test are ended by a sudden increase in force related to the moment the syringe plunger contacts its bottom. The most stable flow was observed for a diameter of 0.84 mm, in which the curve did not show any deviations during the test (Fig. 2A). The fluctuation of the extrusion force can indicate the presence of aggregates by a positive peak, whereas on the other hand, air introduced during the cartridge filling procedure is indicated by a negative peak in the extrusion force (Müller et al., 2019). In the case of AG and CSAG composites, fluctuations may also indicate the commencement of a phase transition if the measurement is conducted at a temperature close to that transition. For AG, regardless of the needle diameter, no negative peaks were registered, which means that the solution was not aerated during production (Fig. 2A). Section B presents the results for CSAG composites obtained based on LMW and MMW CSs (Fig. 2B). It is evident that the extrusion force decreases with an increasing proportion of AG in the composite for both types of chitosan with the studied molecular weights. This suggests that AG can be extruded with less force than CS. This statement is valid because the chitosan hydrogel itself in carbonic acid is unstable over time and will always show positive and negative fluctuations, associated with the escape of carbon dioxide from the gel trapped in excess and the formation of polymer aggregates near the phase transition. LMW CSAG composites show greater fluctuations in extrusion force, which may indicate less uniform material flow through the nozzle compared to MMW CSAG composites, which have a more uniform and stable extrusion force profile, considered in this work as optimal, taking into account the specifics of the designed bioink (Fig. 2B).

3.2. *Biological properties*

3.2.1. *Antimicrobial activity*

To evaluate the antimicrobial activity of materials based on CS, AG, and their composites, ASTM Method E2149 was employed with minor modifications suitable for water-insoluble samples. Fig. 3 illustrates the

MOST WIEDZY Downloaded from mostwiedzy.pl

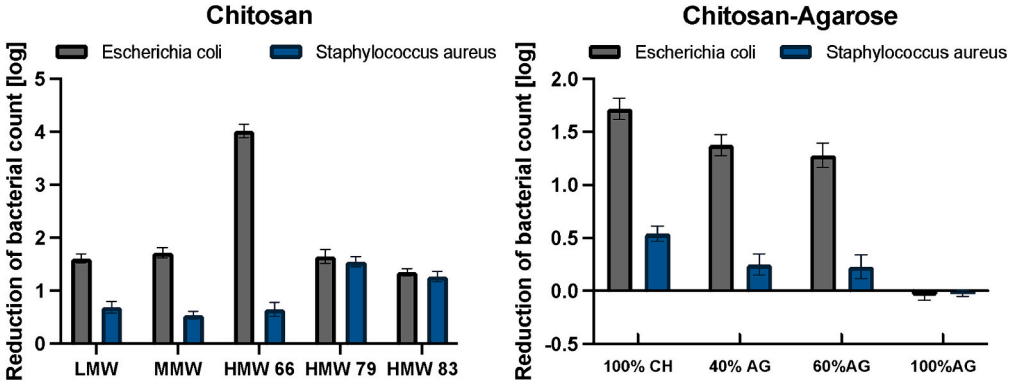

Fig. 3. The antimicrobial activity against *E. coli* and *S. aureus* for (A) CS materials with different MW and DD and (B) CSAG composites according to Standard ASTM: E2149.

antimicrobial activity, expressed as a logarithmic reduction degree after 24 h of interaction between the *Staphylococcus aureus* and *Escherichia coli* inoculum and the materials tested.

The initial phase of the study involved analyzing the impact of CS molecular weight on its antimicrobial effectiveness. This stage aimed to select a potential base material for subsequent investigations into the antimicrobial properties of CSAG composites. Our previous research indicated that CS molecular weight significantly influences its capability to suppress microbial growth (Mania et al., 2023). However, we highlighted that the activity observed might be attributable to sodium hydroxyacetate residues, which notably hinder microbial growth. To confirm these findings, the current study replicated the research with certain modifications. The CS precipitate, acquired through precipitation, underwent a rinse to stable pH of washing water rather than a threefold rinse to potentially remove any sodium hydroxyacetate residues.

The results presented in Fig. 3 reveal globally the higher antimicrobial activity of CSs against Gram-negative than Gram-positive bacteria. The reduction degree for CSs differing the molecular mass (LMW, MMW, and HMW79 with similar DD) is comparably about 1.61–1.72 log against Gram-negative bacteria, and 0.64, 0.59, and 1.55 log reduction for Gram-positive, respectively. In our previous work, we also failed to find a strict relationship between the antimicrobial activity of CSs and their DD (Mania et al., 2023). However, the results in Fig. 3A indicate a trend of decreasing antimicrobial activity with an increasing degree of deacetylation against *E. coli* bacteria. No such trend was observed in the case of *S. aureus*. In the same section, the HMW63 sample is characteristic, demonstrating bactericidal action against *E. coli* and bacteriostatic effect towards *S. aureus*, as a result of the effect of coating bacterial cells with HMW CS, particularly efficient between the cationic polymer and the negatively charged components of the Gram-negative bacterial cell membrane, as well as the chelation mechanism of ions that are part of the cell membranes. According to the literature, this mechanism occurs more frequently at pH $>$ 6.5, due to the ability of the deprotonated amino group to donate a free pair of nitrogen. At pH values of 7–9, the chelation of metal ions occurs both through amino groups and two deprotonated hydroxyl groups, forming a more stable complex than two -NH_2 receptor groups at lower pH (Goy, Britto, & Assis, 2009, Mania et al., 2023). The results prove that the degree of purification of CS from the residual salts formed during its precipitation in the procedure is of great importance. There is no strict relationship between the effect of molecular weight and antimicrobial activity, which may result from the existence of several competing mechanisms of this activity, the effect of which results from the method of preparing the chitosan material and the environment in which this material was placed. In most cases, the effect of pure chitosan can be described as bacteriostatic.

These findings and rheological results led to the selection of MMW CS for further study on CSAG composite activity due to its consistent reduction effect on bacteria. Composite analysis indicated that increasing AG content in the samples correlates with diminished antimicrobial action against both bacterial strains. The CS-based materials exhibited cell reduction rates for *E. coli* and *S. aureus* of 1.72 and 0.54 (98.24 % and 70.71 %), respectively, on a logarithmic scale. At 60 % agarose content, the activity reduced to 1.28 and 0.23 log, equating to 95.88 % and 45.44 %, respectively. Furthermore, it was verified that xerogel materials composed solely of agarose lacked antimicrobial activity (Fig. 3B). The observed decline in activity with increasing agarose is attributed to the diminished chitosan concentration in the final product, the sole polymer with the inherent ability to inhibit both Gram-negative and Gram-positive bacteria in this study.

3.2.2. *Biological safety*

The biological safety of raw materials/biomaterials used in bioprinting is an entry criterion that permits their application in tissue engineering. In the evaluation of medical devices such as implants and other medical or pharmaceutical products, standardized tests for biological safety assessment are employed to capture the entire complexity of the human body. In accordance with the ISO 10993 standard "Biological evaluation of medical devices," a series of recommendations, parameters, and conditions for conducting the test ISO 10993-5:2009 are described, in which the recommended cell line for cell viability studies is the mouse fibroblasts L929 (Jablonská, Kubásek, Vojtěch, Ruml, & Lipov, 2021).

3.2.2.1. MTT assay. Fig. 4A indicates that CS of various molecular weights and DD, as well as AG at each dilution, i.e., 1:1 *v*/v, 1:5 v/v, and 1:9 v/v, do not exhibit a cytotoxic effect on L929 cells. The only significant difference was registered for the sample of high molecular weight chitosan with a DD of 83 %, for which the lowest survival rate was obtained, namely 80 % relative to the control.

HMW83 was characterized by an approximately 7-fold higher molecular weight than the other two high molecular weight chitosans, so such an effect may result from, among other things, different aggregation of the polymer chain, more difficult washing out of hydroxyacetate residues due to the high viscosity of the solution and the nature of the formation of the microcrystalline CS precipitate during its precipitation from the solution (Gorczyca et al., 2014).

These results confirm our earlier hypothesis, as well as the fact that the degree of washing out of the CS precipitate significantly affects the cytotoxicity of the biomaterial, which results from the residues of sodium salts of hydroxyacetic acid (Mania et al., 2013). Control untreated L929 cells and treated with agarose and chitosan extracts resembled the typical morphology (Fig. 4B). Cells exhibited heterogeneous shapes, including: spindle-like, epithelial-like, stellate, and rounded. Some of the cells were bigger and flattened. The morphology of the L929 cells did not change upon treatment with CS and AG extracts. They also did not

MOST WIEDZY Downloaded from mostwiedzy.pl

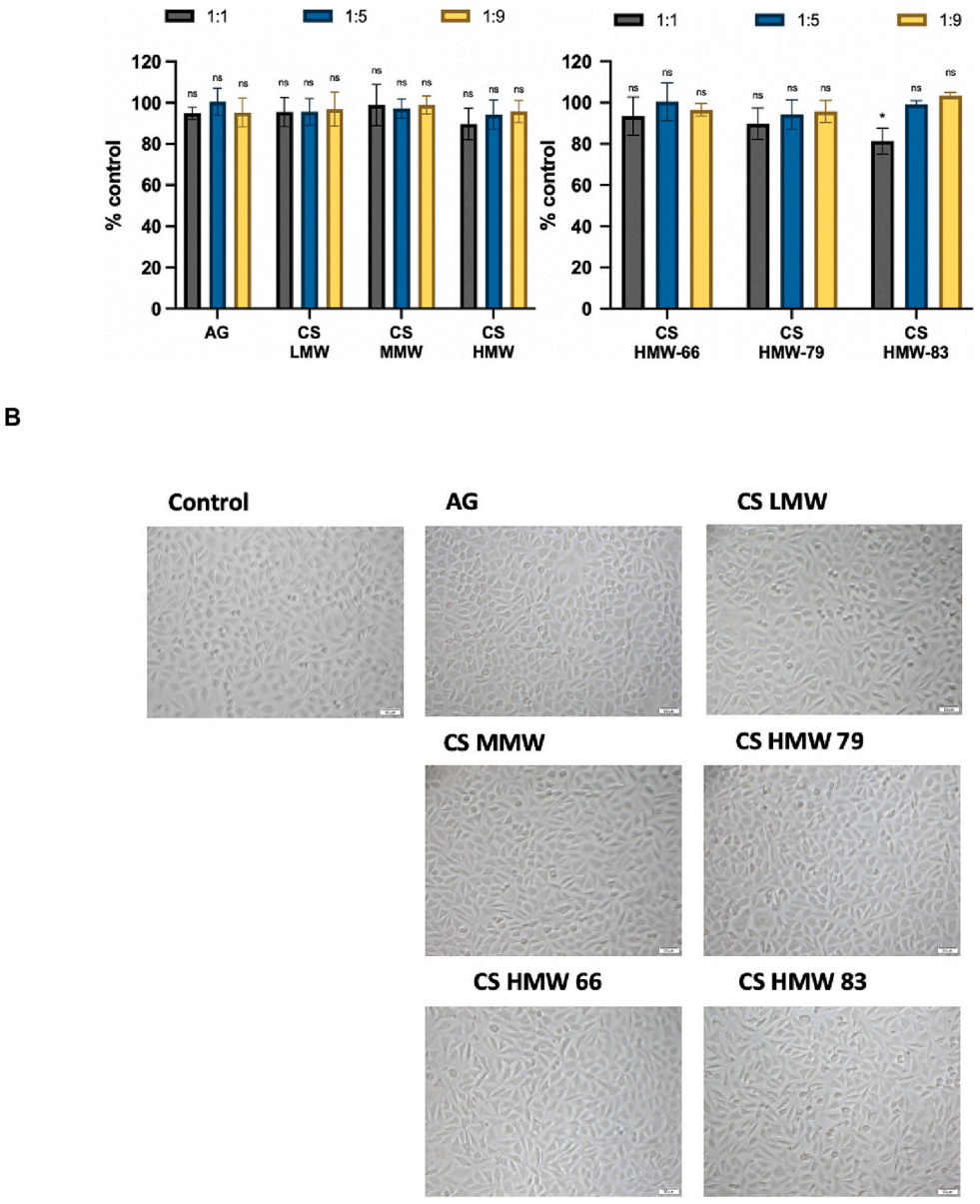

Fig. 4. (A) The cytotoxicity of CS of different molecular weights and AG and (B) CS of different deacetylation degree: 66, 79 and 83 following 24 h incubation against L929 cells. Data are expressed as the mean ± standard deviation of four independent experiments. The results were analyzed by one-way ANOVA with comparisons vs. control: ns (not statistically significant, $p > 0.05$), *$p < 0.05$. B) Representative images ($n = 4$) of the morphology of L929 cells treated with agarose and chitosan extracts dissolved in cell medium. Pictures were taken after 24 h treatment of cells with agarose and chitosan extracts at diluent factor 1:1. Scale bar is 50 μm, magnification 200×.

affect the proliferation of cells. In presented images it is easy to recognize cells undergoing mitosis – they are rounded and more convex, and some of them are still closely situated to each other. In summary, the CS extracts are not harmful to L929 cells. More photos of all dilutions are available in Supplementary materials.

The obtained results are also consistent with our earlier studies, which examined how the developed method for removing endotoxins from chitosan affects the cytotoxicity of its solution. At a 1:1 *v*/v dilution, the survival relative to the control was about 80 % for uncleaned CS of MMW (Banach-Kopeć et al., 2022). In summary, the survival of L929 cells after 24-h contact with CS material obtained by the innovative carbon dioxide saturation method is at least 2.5 times greater, approximately 50 % compared to the control, than in the case of chitosan obtained by dissolving it in 0.1 M lactic acid (Mania et al., 2023). In accordance with ISO standard 10,993–5:2009(E), both materials, i.e., chitosan and agarose, are not cytotoxic and can be safely used in tissue engineering.

3.2.2.2. XTT/LDH assays. Results presented in Fig. 5 confirmed the overall safety and biocompatibility of the analyzed materials. The LDH analysis indicated that CS, AG and CSAG composite did not elicit a cytotoxic effect on human skin cells (HaCaT keratinocytes and 46BR.1 N fibroblasts). In the XTT assay, only the highest concentration (100 %) of AG and CS extracts slightly reduced cell viability (<10 %) in HaCaT keratinocytes. Interestingly, for 46BR.1 N fibroblasts, a significant increase in cell viability was observed. The most pronounced effect (>30 % compared to the control) was noted for CS at 10 % and 25 % concentrations. AG enhanced cell viability by approximately 20 % across all tested concentrations. For CSAG, a 25 % increase in cell viability was observed at a 25 % extract concentration, while all other tested concentrations resulted in a 20 % increase in cell viability.

The absence of cytotoxic effects from agarose-based scaffolds was

MOST WIEDZY Downloaded from mostwiedzy.pl

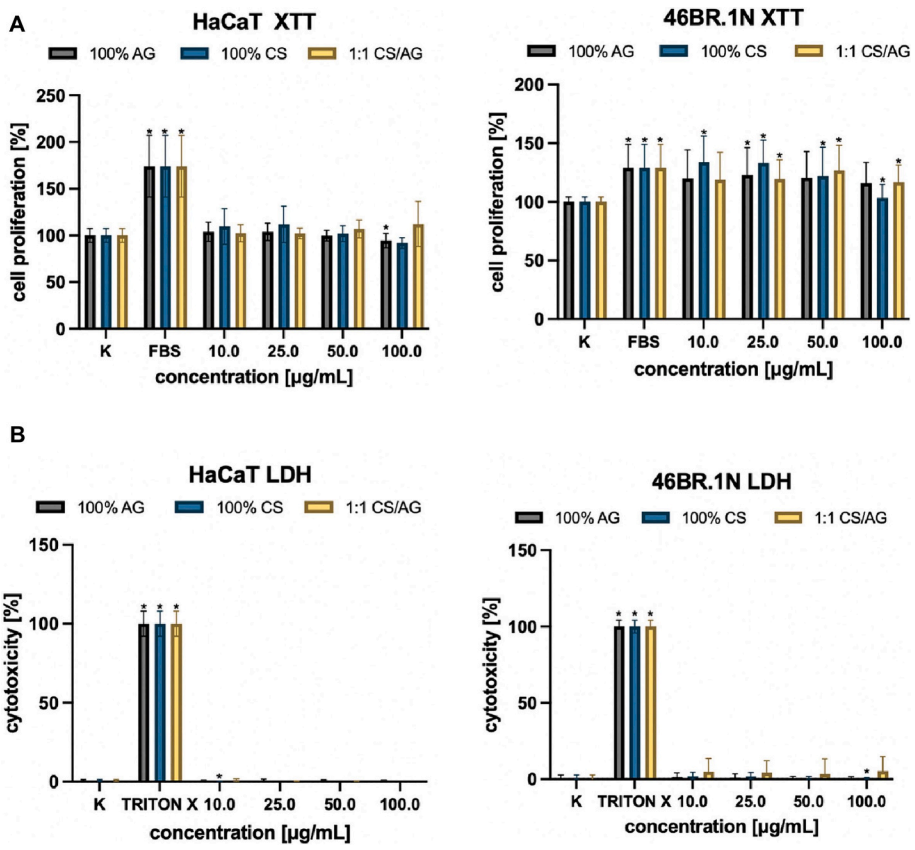

Fig. 5. Effect of CS, AG and CSAG on human skin cells after 48 h of incubation. (A) Xerogels effect on proliferation of HaCaT keratinocytes and 46BR.1 N fibroblasts, (B) Cytotoxicity of the scaffolds towards HaCaT keratinocytes and 46BR.1 N fibroblasts. The graphs show results from three independent experiments. Results are presented as mean with SEM. * - statistically significant differences compared to control, Mann-Whitney *U* test, $p < 0.05$.

also corroborated in the study by Witzler group, where MTT assays on MG-63 osteosarcoma cell lines and Lw35 primary hMSCs revealed no toxic effects of AG (Witzler et al., 2019). However, more extensive research on the biocompatible effects on skin cells has been conducted for chitosan. Indeed, this polymer and its derivatives are crucial in the first three stages of wound healing, notably in promoting the growth of granulation tissue, which consists of inflammatory cells, capillaries, and fibroblasts. The effectiveness varies with the degree of deacetylation and molecular weight, with those possessing a high degree of deacetylation and low molecular weight exhibiting the most beneficial properties. Moreover, fibroblasts can be categorized into two phenotypes: chitosan-responsive and chitosan-non-responsive, which are not influenced by the donor's sex, age, or anatomical site. As for keratinocyte cells, the polymer's effect on their proliferation can be either inhibitory or non-inhibitory, depending on the degree of deacetylation; an increase in deacetylation tends to exhibit an inhibitory effect (Howling et al., 2001). In summary, this study supports our previous assumptions that highly biocompatible materials such as chitosan and agarose can lead to the development of biologically safe biomaterials with potential applications in wound healing, including for burn injuries.

3.2.2.3. Live-dead assay. For an in-depth exploration of the biological safety of the investigated system, additional studies on the viability of HaCaT and 46BR.1 N cell lines were conducted upon integrating them with the bioink base, specifically the CSAG composition at 1:1 mass ratio and 100 % AG serving as the control. The primary objective was to validate the non-cytotoxic nature of the CSAG setup, a finding previously corroborated through research that assessed how extracts from the polymers under investigation affect cytotoxicity and cell proliferation. In this method, the effects of the hydrogel bioink base and thus the hydrogel scaffold on cells after extrusion and after a 48-h incubation period were analyzed. After staining, cell viability was found to remain significantly high in all samples assessed, exceeding 80 % for the 100 % AG formulation and above 90 % for the CS/AG composition (Fig. 6).

This high rate of survival underlines a positive interaction between the studied cells and the bio-ink base, thus confirming the absence of cytotoxic effects. A further step in research to optimise the use of a bio-ink base in cell culture will be to determine how cells proliferate, migrate and survive in the long term. However, achieving this will depend on several variables, such as scaffold porosity, nutrient access and thus scaffold size and geometry. These will be key aspects that will be investigated in the next phase of the research to further understand the interactions between the bio-inks tested and the cells in the context of their biomedical applications.

3.3. Chemical structure

The infrared spectroscopy was used to identify individual chemical groups in pure CS and AG as well as to register structural changes in composites of both polymers (Fig. 7). The CS spectrum shows the labels of the characteristic bands for chitosan. Intense signals at wavelengths of 1151 cm^{-1}, 1064 cm^{-1},1028 cm^{-1} and 898 cm^{-1} indicate the presence of a saccharide structure. Another characteristic bands at 3356 cm^{-1} and 3290 cm^{-1} are the signals coming from the hydroxyl group of the chitosan molecule. A series of signals at 1586 cm^{-1}, 1467 cm^{-1}, 1373 cm^{-1}, and 1317 cm^{-1} correspond to amides I, II and III. The remaining marked signal come from groups -CH_2- (Mania et al., 2018; Staroszczyk, Sztuka, Wolska, Wojtasz-Pająk, & Kołodziejska, 2014). The FTIR spectrum of AG shows a wide band at 3362 cm^{-1}, which is attributed to the stretching vibrations of the -OH groups. The band at 2899 cm^{-1} corresponds to the symmetrical vibrations of the C—H groups. The vibrations at wave numbers 1637 cm^{-1} and 1370 cm^{-1} are bending vibrations -OH and

MOST WIEDZY Downloaded from mostwiedzy.pl

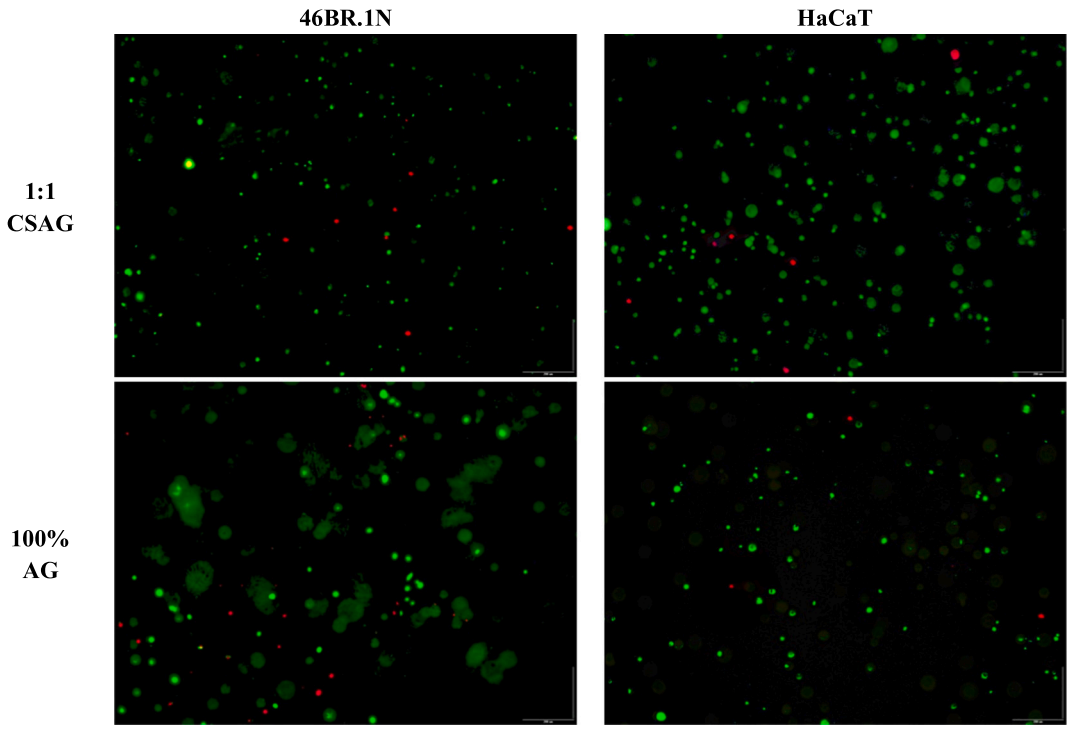

Fig. 6. Viability of 46BR.1 N fibroblasts and HaCaT keratinocytes embedded in CSAG composite and in AG alone. This figure presents fluorescent microscope images showing live-dead staining of cells in the scaffolds at day 2 of cultivation. Viable cells are stained green with calcein, while dead cells are stained red with propidium iodide; the scale bar 250 μm.

C—C, respectively.

The most intense band can be seen at 1039 cm^{-1}. This band is assigned to deformation vibrations of C—O groups in saccharide molecules. The peak at 890 cm^{-1} is attributed to the C—H angular strain of the anomeric carbon of β-galactose and about 930 cm^{-1} to 3,6-anhydrogalactose (Gómez-Mascaraque, Méndez, Fernández-Gutiérrez, Vázquez, & San Román, 2014; Sivashankari & Prabaharan, 2020). The nature of the interactions between CS and AG in their composite containing the same mass fraction of both polymers was also examined. The characteristic peaks were detected as in the spectra of individual components of this composite. The intensity of individual bands is the value resulting from mixing both components in equal proportion. According to literature, some bands of CSAG composite can be shifted against the bands of pure components. This mainly concerns the shift of the chitosan amide II band towards longer wavenumbers, which may be caused by the formation of intermolecular hydrogen bonds between chitosan amino groups and agarose hydroxyl groups (Sivashankari & Prabaharan, 2020; Zamora-Mora, Velasco, Hernández, Mijangos, & Kumacheva, 2014). The spectrum of the composite shows that despite the cationic nature of chitosan and the anionic nature of agarose, mixing their hydrogels allowed to obtain a physical mixture of polymers with very weak hydrogen interactions in the form of physical mixture. The FTIR measurement results also confirm that the presence of agarose in the CSAG composite does not significantly impair its antimicrobial properties resulting from the presence of chitosan due to the presence of weak hydrogen bonds between these polymers. The decrease in the antimicrobial activity of the composite with increasing agarose content is primarily due to the reduced chitosan concentration in the final composite. The hydrogen bonds between chitosan and agarose are insufficiently strong to block the interaction of chitosan with the membranes of both Gram-positive and Gram-negative bacteria.

3.4. 3D bioprinting

In Fig. 8, an attempt to create a 3-layer print in the form of a lattice structure is depicted. The print attempt using chitosan hydrogel was unsuccessful due to the lack of a phase transition in the temperature range defined in rheological studies (Fig. 1A).

Already a 20 % inclusion of AG hydrogel in the bioink was sufficient for successful application of subsequent layers. The increase in agarose content in the bioink was not significant in visual assessment. Only for samples containing at least 80 % agarose hydrogel does the granularity of the print become visible, which may be due to the narrow temperature range of AG phase transition and the beginning of its gelling during flow in the conducted empirical test. However, the same test confirms the possibility of using the proposed CSAG bioink in 3D bioprinting technology.

4. Conclusion

This study successfully develops a printable, thermosensitive bioink composed of medium molecular weight chitosan hydrogel obtained by CO_2 saturation method and agarose hydrogel as a fast-gelling agent. The bioink exhibits pseudoplastic behavior and a favorable sol-gel phase transition temperature, ideal for bioprinting applications. Its antimicrobial properties, demonstrated through significant reduction in *E. coli* and *S. aureus* populations, coupled with its non-cytotoxic nature to various cell lines, establish its potential in advanced spatial cell cultures and tissue engineering. This is the first publication that presents a change in the antimicrobial activity of processed chitosan and, at the same time, free from any acid residues necessary for its dissolution, which is of great importance in the design of new solutions based on this polymer. The research notably advances the field by presenting a novel, safe, and efficient bioink, suitable for creating complex structures in tissue engineering, particularly for skin regeneration. This bioink's characteristics open new avenues for 3D bioprinting technologies, emphasizing the importance of material selection and composition in developing future biomedical applications.

In the context of further perspectives, our research on CSAG bioink in tissue engineering will continue to deeply understand the gelation

MOST WIEDZY Downloaded from mostwiedzy.pl

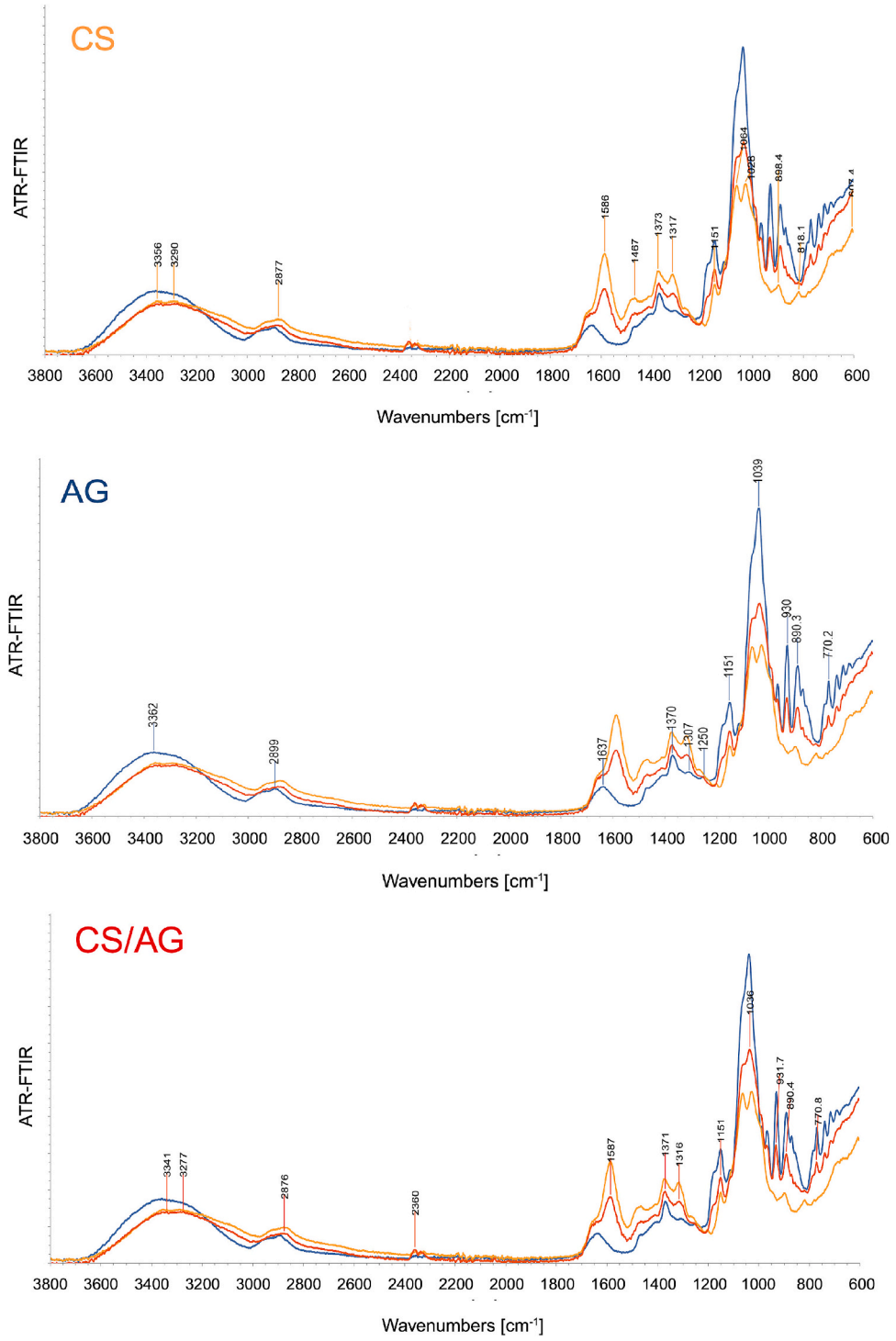

Fig. 7. The ATR-FTIR spectra with labeled signals for CS, AG, and CSAG.

mechanism of agarose in the presence of chitosan. It is necessary to confirm the hypothesis that chitosan contributes to the formation of a more ordered agarose gel structure, which may delay the gelation process and thereby lower the gelation temperature. Additionally, we plan to expand the research to evaluate the applicability of the discussed bioink base in cell cultures by determining the impact of key parameters on both the survivability and printability of the bioink. The next stage will involve advanced studies, both in vivo and in vitro, aimed at a detailed understanding of the interactions between the bioink components and living cells, and their impact on regenerative processes in tissues. Such a comprehensive research program will enable the optimization of the bio-ink composition, which is crucial for its future clinical and industrial applications, ensuring safety and efficacy in creating functional tissue structures.

Funding

Financial support of these studies from Gdańsk University of Technology by the DEC-10/2021/IDUB/I.3.3 grant under the Argentum Triggering Research Grants - 'Excellence Initiative - Research

MOST WIEDZY Downloaded from mostwiedzy.pl

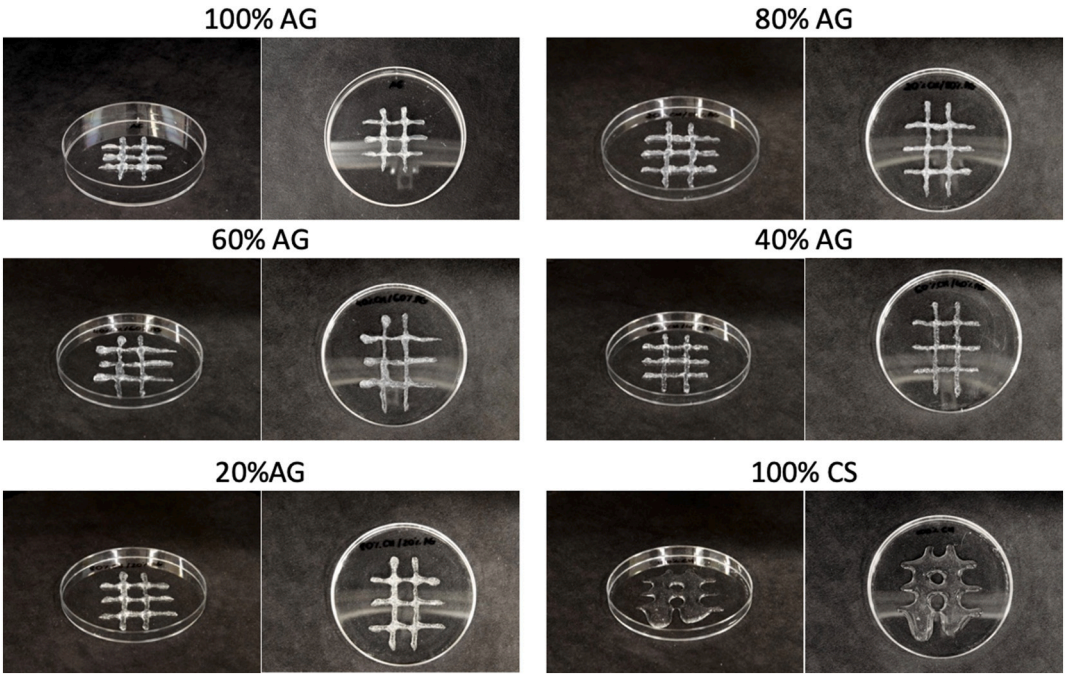

Fig. 8. Results of three-layer 3D prints using CS, AG, and CSAG.

University' program is gratefully acknowledged.

CRediT authorship contribution statement

Adrianna Banach-Kopeć: Writing – review & editing, Writing – original draft, Visualization, Validation, Software, Resources, Methodology, Investigation, Formal analysis, Data curation, Conceptualization. **Szymon Mania:** Project administration, Methodology, Investigation, Funding acquisition, Formal analysis, Data curation, Conceptualization, Resources, Software, Supervision, Validation, Visualization, Writing – original draft, Writing – review & editing. **Robert Tylingo:** Writing – review & editing, Writing – original draft, Validation, Supervision, Software, Methodology, Investigation, Formal analysis, Data curation. **Agata Wawrzynowicz:** Investigation, Data curation. **Monika Pawłowska:** Writing – review & editing, Writing – original draft, Visualization, Validation, Software, Resources, Methodology, Investigation, Data curation. **Katarzyna Czerwiec:** Methodology, Investigation, Data curation, Resources, Software, Validation, Visualization, Writing – original draft, Writing – review & editing. **Milena Deptuła:** Data curation, Investigation, Methodology, Resources, Software, Supervision, Validation, Visualization, Writing – original draft, Writing – review & editing. **Michał Pikuła:** Data curation, Investigation, Methodology, Software, Supervision, Validation, Writing – original draft, Writing – review & editing.

Declaration of competing interest

The authors declare the following financial interests/personal relationships which may be considered as potential competing interests: Szymon Mania reports financial support was provided by Gdansk University of Technology. If there are other authors, they declare that they have no known competing financial interests or personal relationships that could have appeared to influence the work reported in this paper.

Data availability

Data will be made available on request.

Appendix A. Supplementary data

Supplementary data to this article can be found online at https://doi.org/10.1016/j.carbpol.2024.122120.

References

Arifin, N., Sudin, I., Ngadiman, N. H. A., & Ishak, M. S. A. (2022). A comprehensive review of biopolymer fabrication in additive manufacturing processing for 3D-tissue-engineering scaffolds. *Polymers, 14*(10), 2119.

Banach-Kopeć, A., Mania, S., Pilch, J., Augustin, E., Gabriel, I., & Tylingo, R. (2022). A novel method of endotoxins removal from chitosan hydrogel as a potential bioink component obtained by CO2 saturation. *International Journal of Molecular Sciences, 23*, 5505.

Butler, H. M., Naseri, E., MacDonald, D. S., Tasker, R. A., & Ahmadi, A. (2021). Investigation of rheology, printability, and biocompatibility of N,O-carboxymethyl chitosan and agarose bioinks for 3D bioprinting of neuron cells. *Materialia, 18*.

Chakraborty, J., Majumder, N., Sharma, A., Prasad, S., & Ghosh, S. (2022). 3D bioprinted silk-reinforced alginate-gellan gum constructs for cartilage regeneration. *Bioprinting, 28*.

Cheung, R. C. F., Ng, T. B., Wong, J. H., & Chan, W. Y. (2015). Chitosan: An update on potential biomedical and pharmaceutical applications. *Marine Drugs, 13*(8), 5156–5186.

do Amaral Sobral, P. J., Gebremariam, G., Drudi, F., De Aguiar Saldanha Pinheiro, A. C., Romani, S., Rocculi, P., & Dalla Rosa, M. (2022). Rheological and viscoelastic properties of chitosan solutions prepared with different chitosan or acetic acid concentrations. *Foods, 11*(17), 2692.

Doe, J., & Smith, A. (2021). Rheological properties of chitosan and its applications as a pseudoplastic fluid in biomedical engineering: A review. *International Journal of Biological Macromolecules, 165*(Part B), 2185–2197.

Gao, C., Li, Y., Liu, X., Huang, J., & Zhang, Z. (2023). 3D bioprinted conductive spinal cord biomimetic scaffolds for promoting neuronal differentiation of neural stem cells and repairing of spinal cord injury. *Chemical Engineering Journal, 451*.

Gómez-Mascaraque, L. G., Méndez, J. A., Fernández-Gutiérrez, M., Vázquez, B., & San Román, J. (2014). Oxidized dextrins as alternative crosslinking agents for polysaccharides: Application to hydrogels of agarose-chitosan. *Acta Biomaterialia, 10*(2), 798–811.

Gorczyca, G., Tylingo, R., Szweda, P., Augustin, E., Sadowska, M., & Milewski, S. (2014). Preparation and characterization of genipin cross-linked porous chitosan–collagen–gelatin scaffolds using chitosan–CO2 solution. *Carbohydrate Polymers, 102*(15), 901–911.

Goy, R. C., Britto, D., & Assis, O. B. G. (2009). A review of the antimicrobial activity of chitosan. *Polímeros: Ciência e Tecnologia, 19*(3), 241–247.

Graham, S., Marina, P. F., & Blencowe, A. (2019). Thermoresponsive polysaccharides and their thermoreversible physical hydrogel networks. *Carbohydrate Polymers, 207*, 143–159.

MOST WIEDZY Downloaded from mostwiedzy.pl

Gu, Y., Schwarz, B., Forget, A., Barbero, A., Martin, I., & Prasad Shastri, V. (2020). Advanced bioink for 3D bioprinting of complex free-standing structures with high stiffness. *Bioengineering, 7*(4), 1–15.
Himanshu, T., Sandeep, S. M., Avanish, S. P., & Shilpi, C. (2022). Hydrogel based 3D printing: Bio ink for tissue engineering. *Journal of Molecular Liquids, 367*, Article 120390.
Howling, G. I., Dettmar, P. W., Goddard, P. A., Hampson, F. C., Dornish, M., & Wood, E. J. (2001). The effect of chitin and chitosan on the proliferation of human skin fibroblasts and keratinocytes in vitro. *Biomaterials, 22*(22), 2959–2966.
Huang, D.-Y., Zhang, Y., Liu, H., Wu, J.-J., Pan, L.-H., Wu, Y., … Tu, T. (2018). Preparation of chitosan/agarose two-component hydrogels and its water holding and sustained release properties. *Modern Food Science and Technology, 34*(11), 145–150.
Innocenzi, P. (2020). Understanding sol–gel transition through a picture: A short tutorial. *Journal of Sol-Gel Science and Technology, 94*, 544–550.
Jablonská, E., Kubásek, J., Vojtěch, D., Ruml, T., & Lipov, J. (2021). Test conditions can significantly affect the results of in vitro cytotoxicity testing of degradable metallic biomaterials. *Scientific Reports, 11*(1), 6628.
Mandrycky, C., Phong, K., & Zheng, Y. (2017). Tissue engineering toward organ-specific regeneration and disease modeling. *MRS Communications, 7*(3), 332–347.
Mania, S., Banach-Kopeć, A., Staszczyk, K., Kulesza, J., Augustin, E., & Tylingo, R. (2023). An influence of molecular weight, deacetylation degree of chitosan xerogels on their antimicrobial activity and cytotoxicity. Comparison of chitosan materials obtained using lactic acid and CO2 saturation. *Carbohydrate Research, 534*, Article 108973.
Mania, S., Tylingo, R., Augustin, E., Gucwa, K. M., Szwacki, J., & Staroszczyk, H. (2018). Investigation of an elutable N-propylphosphonic acid chitosan derivative composition with a chitosan matrix prepared from carbonic acid solution. *Carbohydrate Polymers, 179*, 196–206.
Müller, M., Fisch, P., Molnar, M., Eggert, S., Binelli, M., Maniura-Weber, K., & Zenobi-Wong, M. (2019). Development and thorough characterization of the processing steps of an ink for 3D printing for bone tissue engineering. *Materials Science and Engineering, C*, Article 110510.
Nordqvist, D., & Vilgis, T. A. (2011). Rheological study of the gelation process of agarose-based solutions. *Food Biophysics, 6*(4), 450–460.
Ramiah, R., du Toit, L., Choonara, Y. E., Kondiah, P. P. D., & Pillay, V. (2020). Hydrogel-based bioinks for 3D bioprinting in tissue regeneration. *Frontiers in Materials, 7*, 76.
Rinaudo, M. (2006). Chitin and chitosan: Properties and applications. *Progress in Polymer Science, 31*(7), 603–632.
Sadeghianmaryan, A., Naghieh, S., Alizadeh Sardroud, H., Yazdanpanah, Z., Afzal Soltani, Y., Sernaglia, J., & Chen, X. (2020). Extrusion-based printing of chitosan scaffolds and their in vitro characterization for cartilage tissue engineering. *International Journal of Biological Macromolecules, 164*, 3179–3192.
Salati, M. A., Khazai, J., Tahmuri, A. M., Samadi, A., Taghizadeh, A., Taghizadeh, M., … Mozafari, M. (2020). *Polymers agarose-based biomaterials: Opportunities and challenges in cartilage tissue engineering*.
Sivashankari, P. R., & Prabaharan, M. (2020). Three-dimensional porous scaffolds based on agarose/chitosan/graphene oxide composite for tissue engineering. *International Journal of Biological Macromolecules, 146*, 222–231.
Smith, J., & Doe, A. (2022). The impact of shear rate on bio-ink printability and cell viability in 3D bioprinting. *Journal of Biomedical Materials Research, 58*(4).
Staroszczyk, H., Sztuka, K., Wolska, J., Wojtasz-Pająk, A., & Kołodziejska, I. (2014). Interactions of fish gelatin and chitosan in uncrosslinked and crosslinked with EDC films: FT-IR study. *Spectrochimica Acta Part A-Molecular and Biomolecular Spectroscopy, 117*, 707–712.
Tan, S. H., Ngo, Z. H., Sci, D. B., Leavesley, D., & Liang, K. (2022, February). Recent advances in the design of three-dimensional and bioprinted scaffolds for full-thickness wound healing. *Tissue Engineering Part B: Reviews, 2022*, 160–181.
Tylingo, R., Kempa, P., Banach-Kopeć, A., & Mania, S. (2022). A novel method of creating thermoplastic chitosan blends to produce cell scaffolds by FDM additive manufacturing. *Carbohydrate Polymers, 280*, Article 119028.
Unagolla, J. M., & Jayasuriya, A. C. (2020). Hydrogel-based 3D bioprinting: A comprehensive review on cell-laden hydrogels, bioink formulations, and future perspectives. In *, Vol. 18*. *Applied materials today*. Elsevier Ltd.
Witzler, M., Ottensmeyer, P. F., Gericke, M., Heinze, T., Tobiasch, E., & Schulze, M. (2019). Non-cytotoxic agarose/hydroxyapatite composite scaffolds for drug release. *International Journal of Molecular Sciences, 20*(14), 3565.
Wu, J., Han, Y., Fu, Q., Hong, Y., Li, L., Cao, J., … Qian, Q. (2022). Application of tissue-derived bioink for articular cartilage lesion repair. *Chemical Engineering Journal, 450*.
Zamora-Mora, V., Velasco, D., Hernández, R., Mijangos, C., & Kumacheva, E. (2014). Chitosan/agarose hydrogels: Cooperative properties and microfluidic preparation. *Carbohydrate Polymers, 111*, 348–355.
Zarrintaj, P., Manouchehri, S., Ahmadi, Z., Saeb, M. R., Urbanska, A. M., Kaplan, D. L., & Mozafari, M. (2018). Agarose-based biomaterials for tissue engineering. *Carbohydrate Polymers, 187*, 66–84.
Zaszczyńska, A., Moczulska-Heljak, M., Gradys, A., & Sajkiewicz, P. (2021). Advances in 3D printing for tissue engineering. *Materials, 14*(12), 3149.
Zhang, X., Chen, X., Hong, H., Hu, R., Liu, J., & Liu, C. (2021). Decellularized extracellular matrix scaffolds: Recent trends and emerging strategies in tissue engineering. *Bioactive Materials, 10*, 15–31.
Zhang, Y., Zhou, D., Chen, J., Zhang, X., Li, X., Zhao, W., & Xu, T. (2019). Biomaterials based on marine resources for 3D bioprinting applications. *Marine Drugs, 17*(10), 555.

MOST WIEDZY Downloaded from mostwiedzy.pl